Journal of Achievements in Materials and Manufacturing Engineering
VOLUME 55
ISSUE 2
December
2012

# Investigation of various properties of monocrystalline silicon solar cell

**L.A. Dobrzański [a], M. Musztyfaga [a,*], M. Giedroć [a], P. Panek [b]**
[a] Institute of Engineering Materials and Biomaterials,
Silesian University of Technology, ul. Konarskiego 18a, 44-100 Gliwice, Poland
[b] Institute of Metallurgy and Materials Science, Polish Academy of Sciences,
ul. Reymonta 25, 30-059 Kraków, Poland
* Corresponding e-mail address: malgorzata.musztyfaga@polsl.pl

Received 21.10.2012; published in revised form 01.12.2012

Properties

## ABSTRACT

**Purpose:** The aim of the paper was to apply Sherescan instrument, which is a valuable tool used for fault detection, error diagnosis and process optimization by cell manufacturers, paste suppliers, institutes and universities all over the world.

**Design/methodology/approach:** Screen printed front side contacts and next to co-fired them in the infrared conveyor furnace were carried out at 920°C temperature. A commercial silver paste to form front side metallization was apply into investigations. The investigations were carried out on monocrystalline silicon wafers. Front side metallization of solar cell was formed on textured surface with coated antireflection layer. Investigated were both surface topography and cross section of front contacts using the SEM microscope. The size of textured silicon surface was measured using the AFM microscope. The thickness of tested front contacts was measured using SEM and CLSM microscope. The metal resistance of solar cells was investigated using the 'Sherescan' instrument. The I-V characteristics of solar cells were also investigated.

**Findings:** The technological recommendations for the co-firing technology in order to produce a uniformly melted structure, well adhering to the substrate, with the low resistance of the front electrode-to-substrate joint zone.

**Research limitations/implications:** The resistance of the metal-semiconductor connection zone depends on conductive paste composition from which the paths were made, as well as manufacturing conditions.

**Originality/value:** The influence of the obtained front side metallization features on electrical properties of solar cell was estimated.

**Keywords:** Electrical properties; Solar cells; Screen printing; Sherescan instrument

**Reference to this paper should be given in the following way:**
L.A. Dobrzański, M. Musztyfaga, M. Giedroć, P. Panek, Investigation of various properties of monocrystalline silicon solar cell, Journal of Achievements in Materials and Manufacturing Engineering 55/2 (2012) 307-315.

## 1. Introduction

Due to the continuously growing population, as well as economic development there is increasing demand for electricity. However, the traditional mass combustion of fossil fuel as dry: coal and crude oil causes a number of serious significant environmental problems such as the ozone hole, greenhouse effect and acid rain. The development of carbon free energy sources is an important aspect of the modern economy. Factors that necessitate the development of renewable technology are environmental protection, increased importance of conventional energy sources, legislation, government policy. There are many different developing renewable energy sources, which replace fossil fuels. Great interest in the production of electricity has an photovoltaic effect. Solar cells are used to convert solar energy into an electricity. The development of photovoltaic began in the sixties of the twentieth century, initiated by the space research, and accelerated by the oil crisis. Photovoltaic power is measured in watts peak power under standard test conditions STC - solar radiation spectrum AM 1.5 (Air Mass 1.5 is the apparent distribution of the Sun 42°), the intensity of radiation Pin = 1000 W/m$^2$ and a temperature T = 288 K [1,2].

Due to the low cost of ownership and simplicity photovoltaic systems are ideal for supply both the objects that are outside of the network and connected to it [3,4]. In recent years the photovoltaic industry is one of the fastest growing industries and the dynamics of its growth is comparable to the development of the microelectronics industry in the early days of its prosperity [5]. The classification of different types of solar cells is shown in Fig. 1 [6]. Monocrystalline silicon is best known as representative of the semiconductor materials family, because it is the base material in the production of microelectronic devices.

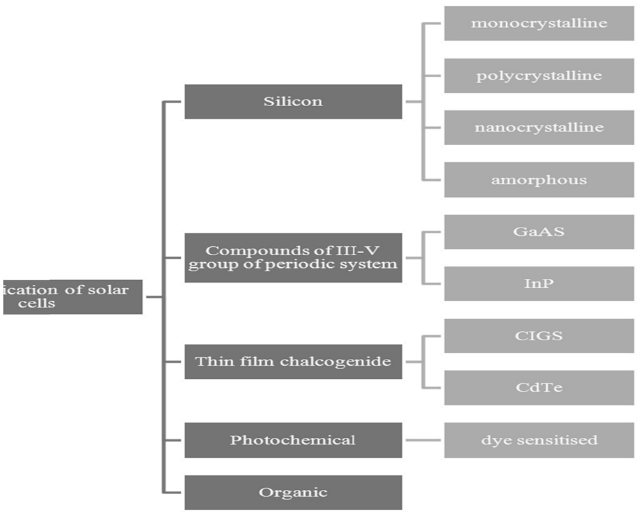


Fig. 1. An example classification of solar cells [5]

The main advantages of silicon solar cells are the following:

- high efficiency (up to 25%),
- the possibility of using the experience of well-developed electronics industry,
- unlimited resources of the starting material,
- simplicity and very good stability,
- good compliance with environmental protection requirements.

Electrical properties of different types of solar cells are shown in Table 1. Crystalline silicon (including monocrystalline and polycrystalline silicon) due to the possibility of receiving from it high efficient (up to 25%) and low-cost terrestrial solar cells is the dominant material in production of solar cells, which occupies more than 80 per cent share of photovoltaic market [7].

Monocrystalline silicon solar cells have the highest conversion efficiency of all silicon solar cells, while production of the large cylindrical ingots which they are made of are the most expensive.

Polycrystalline silicon solar cells are less efficient than monocrystalline solar cells, but their cost of production is also lower, due to the omission of the energy-consuming step of manufacture of a single crystal. Therefore, polycrystalline silicon solar cells occupy over 50 per cent share of photovoltaic market [8,9].

Stages of an example production technology of conventional silicon solar cells are as follows [10]:

- preparation of silicon surface,
- the creation of p - n junction,
- passivation of silicon surface,
- deposition of anti-reflection layer,
- applying electrical contacts by for example: screen printing or selective laser sintering method.

Surface condition has a huge impact on the efficiency of silicon solar cells. The first stage in production technology of conventional silicon solar cells is to remove from the wafers damage surface layer, which is a result of cutting the silicon block (in case of polycrystalline silicon) or large cylindrical ingots (in case of monocrystalline silicon) to make wafer. For this purpose, silicon wafers are degreased, cleaned (in solution such as hydrochloric acid or potassium hydroxide) and polished (for example mechanically or chemically). As a result of this treatment approximately 15 µm silicon layer is removed from both sides.

Then, in order to reduce the reflectance, silicon wafers are subjected to surface texturing. It is a commonly used step in production of conventional silicon solar cells that improves the efficiency of photovoltaic cells by forming microscopic pyramid on the surface of silicon wafers [11-13].

Generally, the p-n junction is formed by dopant diffusion (typically the donor) to the base plate (type p) by one of its surfaces [14,15].

The next step is to remove impurities from the edge of the donor and phosphorous silicate glass from the surface of the wafer, which were created during the diffusion, by chemical etching and dip in the acid solutions. Passivation of the silicon surface is performed in order to reduce the losses caused by surface recombination. This is achieved by surface passivation using a $SiO_2$ layer [16].

Subsequently, antireflective layer is deposited onto silicon surface wafer in order to reduce light reflection.

Last step in production of silicon solar cells is to perform electrical contacts by convectional (for example screen printing) or unconventional method (for instance, selective laser sintering). Screen printed method is a technique in which electrical contacts are applied on the surface by overprint, next they are drying into the dryer and co-firing in the furnace [17-20]. Selective Laser Sintering (SLS) is using a high-power $CO_2$ laser to melt or sinter, metal powder particles onto the surface of silicon wafer [21-23]. The example construction of silicon solar cell is shown in Fig. 2.

In order to realize efficient and cost effective solar cells with minimum losses it is important to measure their electrical properties on special research devices.

The Sherescan instrument, which is one of the latest equipment available on the market, is used to optimize, control and diagnose production processes of photovoltaic cells. The Sherescan instrument offers three modes of measurement [24-28]:

- emitter sheet resistance across the surface of a single wafer,
- P/N recognition,
- metal conductivity.

The scanning electron microscope (SEM) and confocal laser scanning microscope (CLSM) are used to investigate topography of both surface and cross section of front contact in order to determine quality of connection of silicon substrate with electrodes.

In order to obtain topography of silicon wafer with texture and electrode the atomic force microscope (AFM) is used.

Output electrical properties of photovoltaic cell is usually determined from the light and dark current - voltage (I-V) characteristics (Fig. 3).

The main objective of present work is to investigate various metallographic and electrical properties of monocrystalline silicon solar cells where the front and back side of metallization was made by screen printed method.

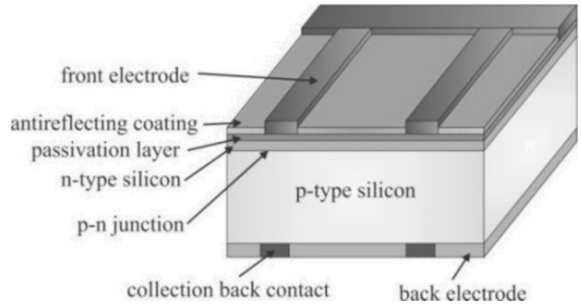


Fig. 2. Construction of conventional silicon solar cell [1]

## 2. Experimental procedure

The photovoltaic cells were performed from monocrystalline silicon p type boron doped in a form of wafers of 200 µm thickness and the area of 25 $cm^2$ with the crystallographic orientation of (100), the resistivity of ~1 Ω·cm and the charge carrier lifetime of ~20 µs. Front metallization was performed from silver PV 145 paste produced by Du Pont company. Connecting back contacts were performed from PV 124 paste with the bismuth glaze and 2% addition of aluminum produced by Du Pont company. Back side metallization was printed from aluminum CN53-101 paste produced by Ferro company.

In the Institute of Metallurgy and Materials Science in Krakow (Poland) was performed Technology of producing solar cells. Fig. 4 presents the process steps for manufacturing solar cells.

Table 2 present the conditions of co-firing solar cells in the conveyor belt IR furnace, which was equipped with fitted tungsten filament lamps, heating both the top and bottom of the belt (Fig. 5).

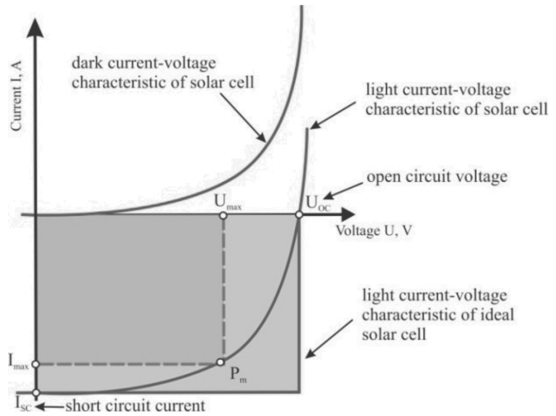


Fig. 3. I-V curve of solar cell [1]

In this paper the following investigations were performed:

- The topography of both surface and cross section of front contacts using:
  - Zeiss Supra 35 scanning electron microscope (SEM) using secondary electron detection with accelerating voltage in the range 5-20 kV.
  - Zeiss confocal laser scanning microscope 5 (CLSM) in which the source of light was a diode laser about power 25 mW emits radiation about wave length 405 nm. The thickness of tested front electrodes was measured using SEM and CLSM.
- The topography of silicon wafer with texture using the atomic force microscope (Park Systems XE 100) in the non-contact mode. The medium size of the pyramids was also measured using this microscope.
- Electrical properties of solar cells (for instance: efficiency, fill factor of solar cell) using the system for measuring the current-voltage characteristic.
- Electrical properties of solar (for instance: sheet resistance, metal resistance) cells using the Sherescan instrument produced by SunLab BV a daughter company of ECN Solar Energy research Centre of the Netherlands.

Table 1.
Electrical properties of different types of solar cells measured under the global AM1.5 at 25°C [6]

| Classification | Efficiency, % | Area, $cm^2$ | $V_{oc}$, V | $I_{sc}$, mA/$cm^2$ | FF, % |
|---|---|---|---|---|---|
| Monocrystalline | 25.0±0.5 | 4.00 | 0.706 | 42.7 | 82.8 |
| Polycrystalline | 20.4±0.5 | 1.002 | 0.664 | 38.0 | 80.9 |
| Nanocrystalline | 10.1±0.2 | 1.199 | 0.539 | 24.4 | 75.5 |
| Amorphous | 10.1±0.3 | 1.036 | 0.886 | 16.75 | 67 |
| GaAs | 28.3±0.8 | 0.9944 | 1.107 | 29.47 | 86.7 |
| InP | 22.1±0.7 | 4.02 | 0.878 | 29.5 | 85.4 |
| CIGS | 19.6±0.6 | 0.996 | 0.713 | 34.8 | 79.2 |
| CdTe | 16.7±0.5 | 1.032 | 0.845 | 26.1 | 75.5 |
| Dye sensitised | 11.0±0.3 | 1.007 | 0.714 | 21.93 | 70.3 |
| Organic | 10.0±0.3 | 1.021 | 0.899 | 16.75 | 66.1 |

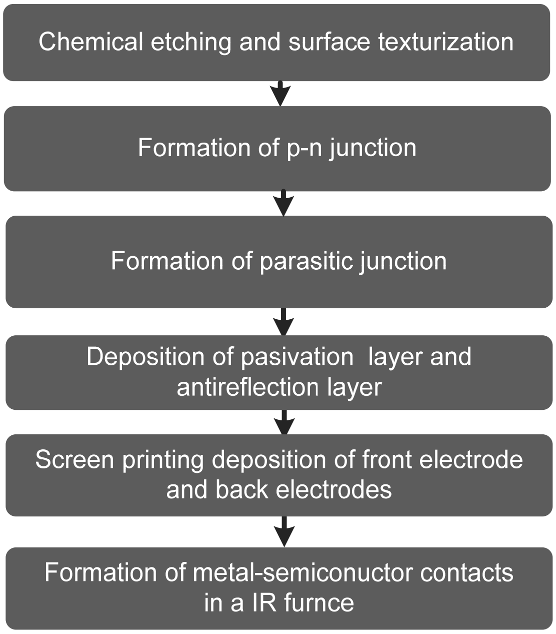


Fig. 4. Scheme of technological manufacturing process of silicon solar cell

Table 2.
Conditions of co-firing in the furnace silicon solar cells (the thickness of front side metallisation - 15 µm)

| Sample symbol | Temperature, °C | | |
|---|---|---|---|
| | Zone I | Zone II | Zone III |
| A | 530 | 580 | 920 |

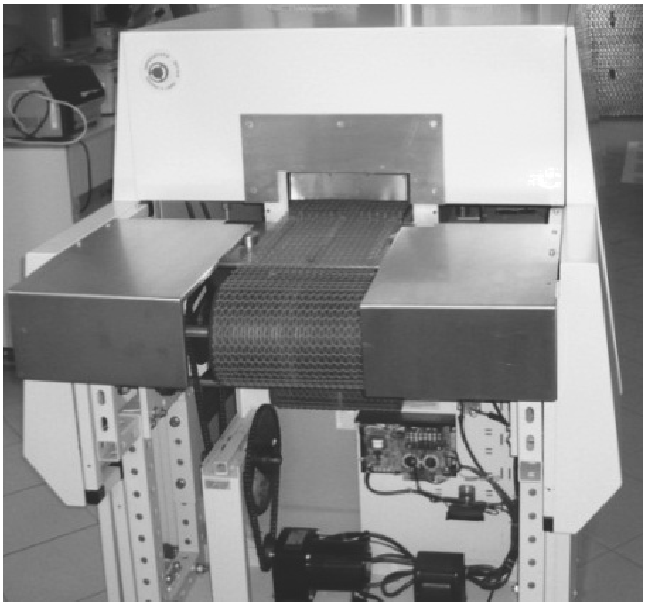

Fig. 5. LA-310 RTC type IR furnace at IMMS PAS

## 3. Results and discussion

It was found based on metallographic observations in the scanning electron microscopy that front contacts obtained from silver PV 145 paste and co-fired in the furnace show a porous structure (Fig. 6). Based on the fractographic investigations, it was found that test electrodes obtained from standard paste PV 145 by co-fired in the conveyor furnace method demonstrated connection with substrate without defects and delaminations. Electrode layer creates many homogenous connections with the silicon substrate, which are close to continuous connection (Fig. 7).

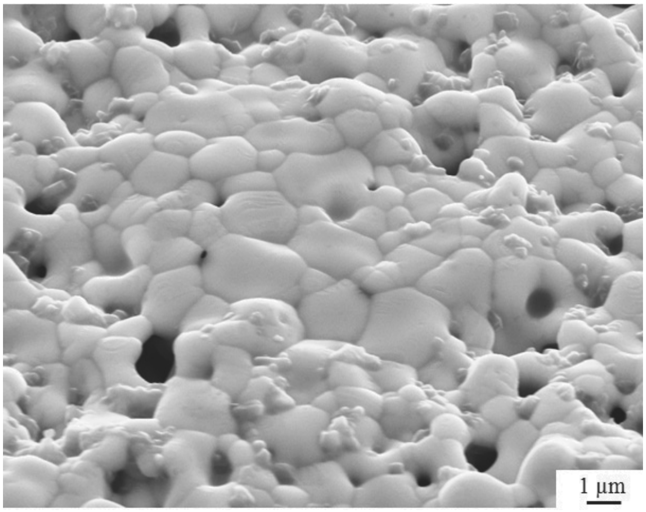


Fig. 6. SEM image of front contact layer co-fired in the furnace at the 920 °C temperature from PV 145 paste on Si substrate with texture and antireflection layer

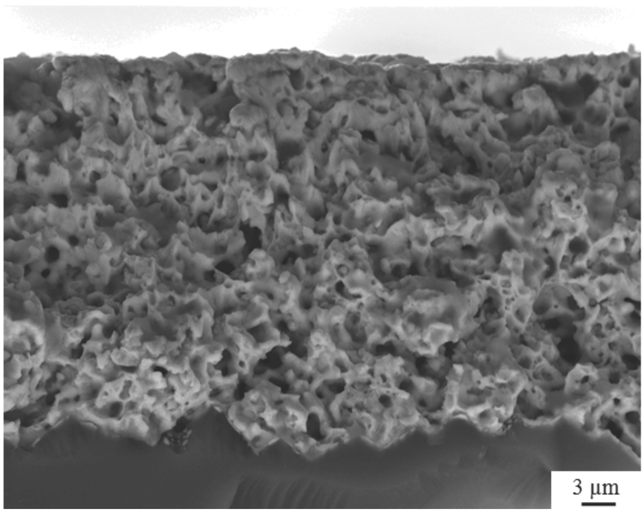


Fig. 7. SEM fracture image of front contact layer co-fired in the furnace at the 920 °C temperature from PV 145 paste on Si substrate without texture and with antireflection layer

The thickness of test electrodes was determined based on the measurement of profile height three dimensional surface topography in the confocal scanning microscope (Fig. 8). The thickness measurement results of the front contacts obtained by co-firing in the furnace on textured silicon substrates are presented in Table 3. The thickness of test contacts co-fired at 920ºC temperature from PV 145 decrease little by little with relation to thickness of electrode before their co-firing. As a result of SEM investigations, the investigated test front side metallization co-fired show the thickness on cross-section in the range from 12 µm to 15 µm.

Topography of silicon wafer was observed with texture in the atomic force microscope. A medium height of pyramids was equal to 3 µm (Fig. 9).

Topography of front electrode was also observed in the atomic force microscope. A medium height of electrode was equal to 2.4 µm (Fig. 10).

Electrical properties of solar cell (Fig. 11, Tab. 4), with front contacts obtained from PV 145 paste, co-fired in the furnace in the 920 °C temperature, determined from I-V curves let confirmed that its efficiency is equal to $E_{ff}$ = 14.98 % and fill factor is equal to FF= 0.765 (Tab. 4). In solar cell with the following reduced short circuit current value was obtained ($I_{sc}$) of 823.87 mA and open-circuit voltage ($U_{oc}$) of 0.59 mV. Electrical properties determined from IV curves using two diode model let ascertain that the factor $A_1$ value equals 1 for all calculations, however the factor $A_2$ value equals 2.50, however the factor ε value equals 0.39%, this confirms the medium unanimity of fitting experimental curve to the theoretical one. It was found based on measurements that series resistance of photovoltaic cell co-fired in the furnace from PV 145 paste in the 920°C temperature equals 0.08 Ω, however the value of dark current, that is $I_{s1}$ equals $3.32^{e-11}$ and $I_{s2}$ equals $4.90^{e-5}$.

As a result of measurement using Sherescan instrument was obtained P - type of silicon wafer. Test result agrees with the type of the silicon wafer purchased from the manufacturer. The sheet resistance measurements obtained in the investigations are presented in Table 5. Solar industry has produced a resistance emitter layer in the range of 45 - 60 Ω/γ.

The panel of Sherescan instrument was introduced the following date: step size 1.5 mm, number of steps 6, metal width in turn and height 0.12 mm and 15µm. During investigation the sheet resistance, and also the specific resistivity of the metal were calculated (Table 6).

Table 3.
Comparison of thickness of front electrodes deposited from PV 145 paste on textured surface with deposited $TiO_x$ coating and co-fired in the furnace

| Sample symbol | Co-firing temperature [°C] III zone | The medium thickness of electrode [µm] | | |
|---|---|---|---|---|
| | | SEM | SEM | CLSM |
| | | Before co-firing | after co-firing | |
| A | 920 | 15 | 13 | 12 |

## 4. Conclusions

It was found based on the metallographic observations that the morphology of front side metallization deposited from paste PV 145 and co-fired in the furnace shows a porous structure. It was found based on the observations in the atomic force microscope that a medium height of pyramids is equal to 3 µm. As a result of SEM and CLSM investigations, the investigated test front contacts co-fired show the thickness on cross-section is equal 12 µm. On the basis of electrical properties investigations using Sherescan instrument it was found that in the 920°C temperature the specific resistivity of contact is equal 0.45 µΩcm² and the sheet resistance of metal contact is equal 0.3 mΩ/□ onto textured substrate having coated antireflection layer of silicon solar cell. Solar generation of high - resistive emitter at 60-80 Ω/γ, characterized by cell quantum efficiency improvement in the wavelength range 400 - 600 nm radiation generates photo-current which directly effect on the growth of photo-conversion efficiency of solar cells.

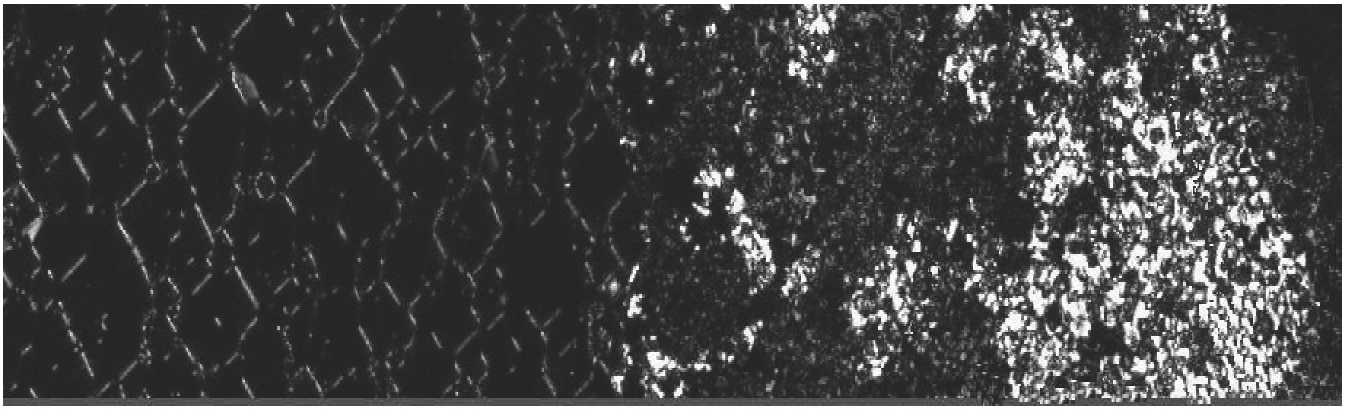

Fig. 8. Two - dimensional surface topography (CLSM) of the front electrode prepared from the PV 145 paste on a surface with texture and with antireflection layer co - fired in the furnace at 920°C temperature (example)

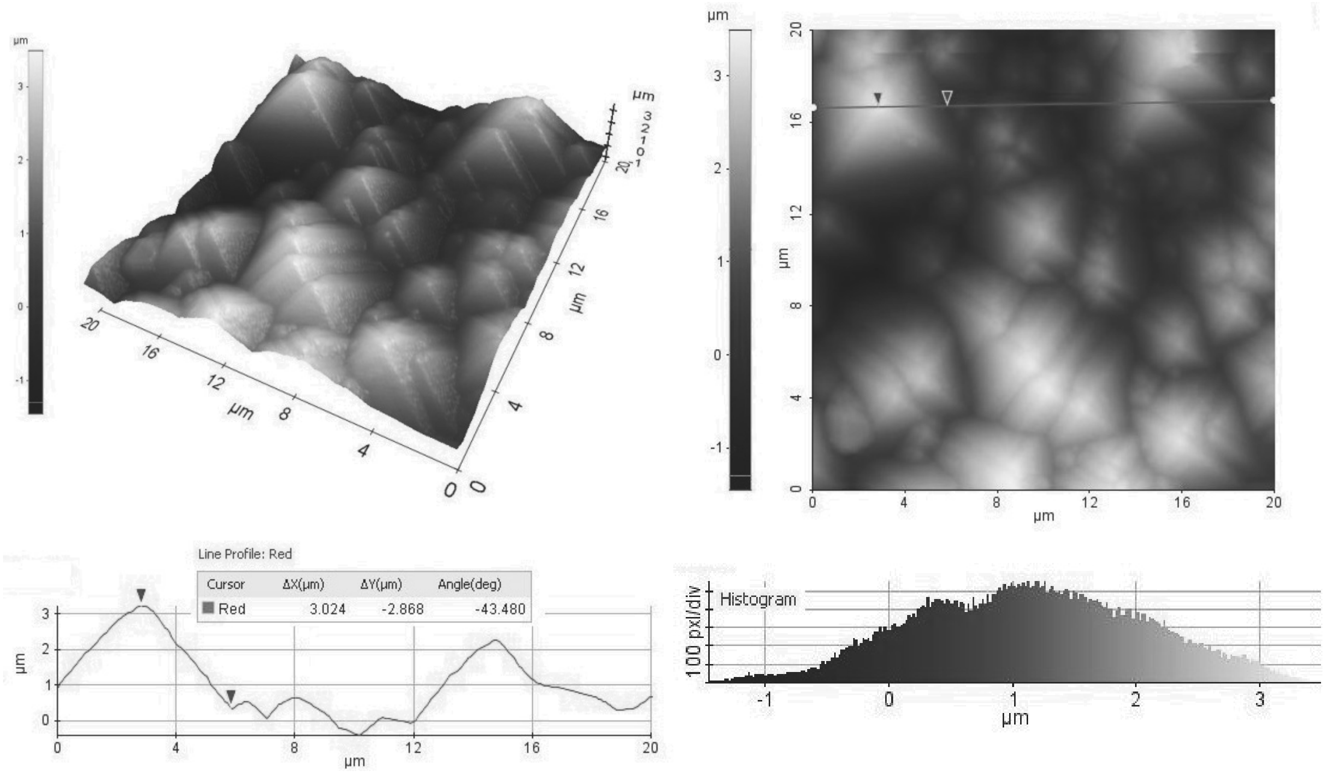


Fig. 9. Topography of the textured surface of monocrystalline solar wafer with thickness 200 µm (AFM)

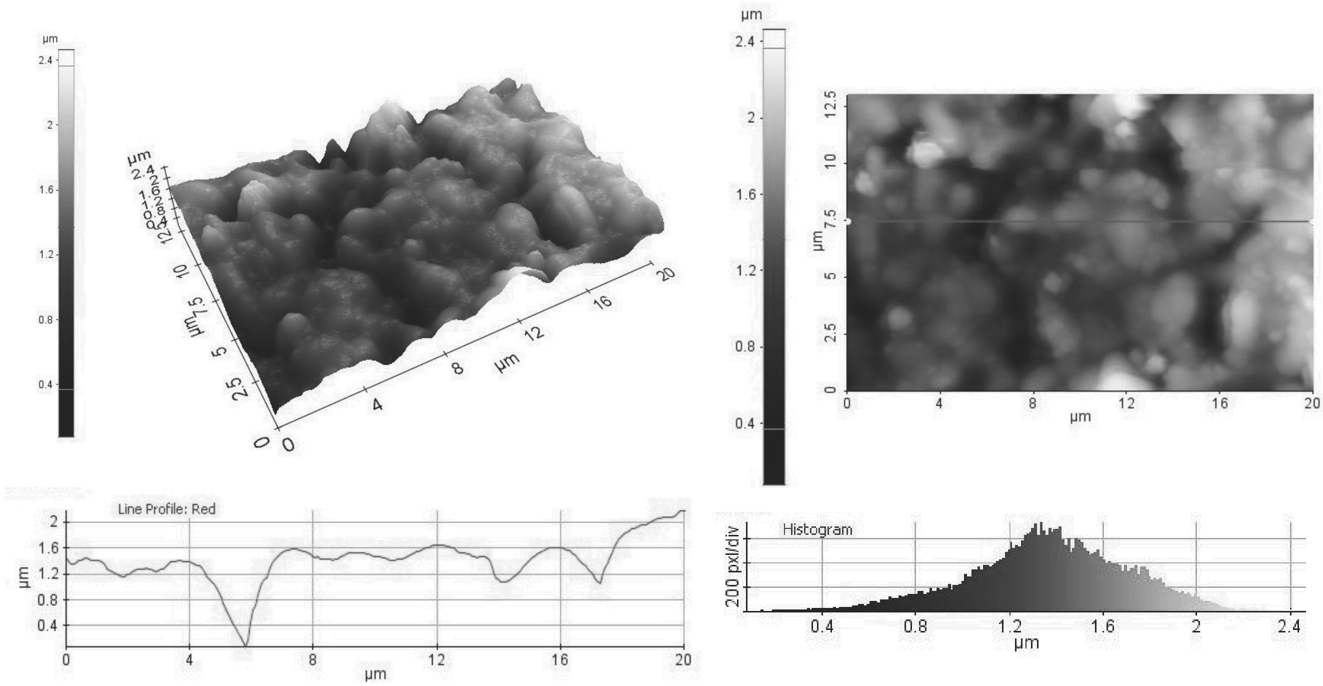


Fig. 10. Topography of front electrode of solar cell (AFM)

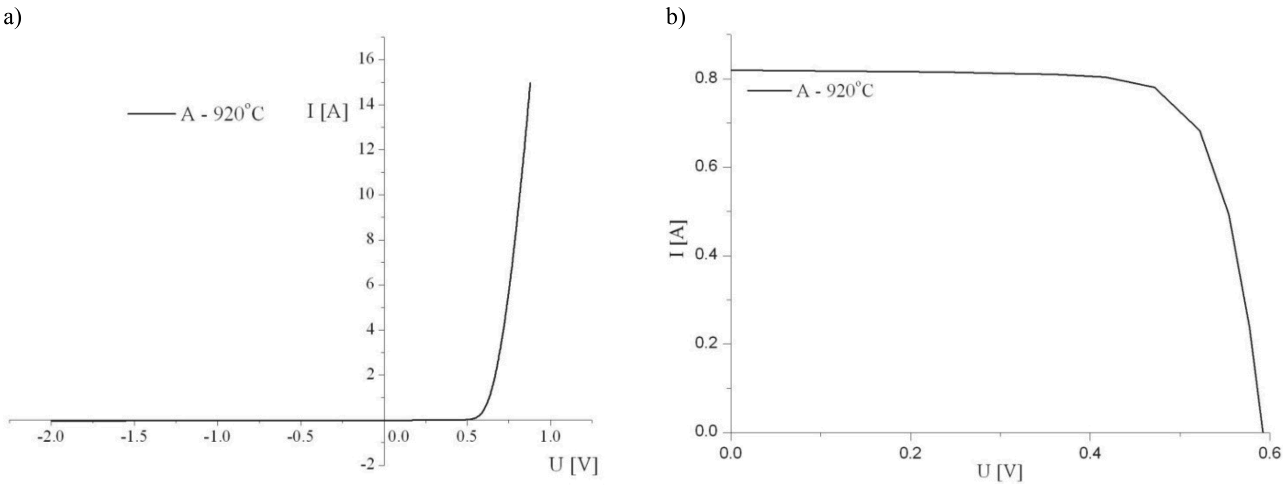


Fig. 11. I-V curve of solar cell co-fired at 920 °C temperature in furnace from PV 145 paste, where: a) dark, b) light curve

Table 4.
Electrical properties of silicon solar cell co-fired in furnace

| Solar cell symbol | Co-firing temperature [°C] | Electrical parameters | | | | | | | |
|---|---|---|---|---|---|---|---|---|---|
| | | $U_{oc}$ [mV] | $I_{sc}$ [mA] | $I_m$ [mA] | $U_m$ [mV] | P [mW] | FF | | $E_{ff}$ [%] |
| Photovoltaic solar cell textured surface with coated antireflection layer | | | | | | | | | |
| A | 920 | 0.5941 | 823.874 | 784.978 | 0.4769 | 374.386 | 0.765 | | 14.98 |
| | | $I_p$ [mA] | $R_{sh}$ [Ω] | $R_s$ [Ω] | $I_{s1}$ [A] | $I_{s2}$ [A] | $A_1$ | $A_2$ | ε [%] |
| | | 860.54 | 12.12 | 0.08 | 3.32e-11 | 4.90e-5 | 1 | 2.50 | 0.39 |

$I_{sc}$ - short circuit current of solar cell, $I_m$ - a current in maximum power point of solar cell, $U_m$ - a voltage in maximum power point of solar cell, $U_{oc}$ - open-circuit voltage of solar cell, FF - fill factor of solar cell, P - power of solar cell, $E_{ff}$ - efficiency of solar cell, $R_{sh}$ - parallel resistance of solar cell, $R_s$ - series resistance of solar cell, $I_{s1}$ - saturation current (diode $D_1$) ingredient of the diffusion dark current, $I_{s2}$ - saturation current (diode $D_2$) ingredient of the generative recombinant dark current, $A_{1,2}$ - diode quality factors, ε - fitting factor, which determines an accuracy of fitting experimental IV curve to theoretical in two diode model of photovoltaic solar cell. It is equal to the difference of surface between the experimental and theoretical curves with relation to surface described by the experimental curve between I and V axes

Table 5.
The sheet resistance measurements

| Solar cell symbol | Co-firing temperature [°C] | Sheet resistance [Ω/□] | | | | |
|---|---|---|---|---|---|---|
| | | Average | Standard deviation | Median | Maximum | Minimum |
| A | 920 | 49.7 | 0.2 | 49.7 | 49.9 | 49.5 |

Table 6.
The metal resistance measurements

| Solar cell symbol | Co-firing temperature [°C] | Specific resistivity of metal | |
|---|---|---|---|
| | | Sheet resistance of metal [mΩ/□] | Specific resistivity of metal [μΩcm$^2$] |
| A | 920 | 0.298 | 0.447 |

## Acknowledgements

Małgorzata Musztyfaga is a holder of scholarship from project POKL.04.01.01-00-003/09-00 entitled „Opening and development of engineering and PhD studies in the field of nanotechnology and materials science" (INFONANO), co-founded by the European Union from financial resources of European Social Fund and headed by Prof. L.A. Dobrzański.

Marzena Giedroć is holder of the "DoktoRIS - Scholarship program for innovative Silesia" co-financed by the European Union under the European Social Fund.

## References

[1] G. Jastrzębska, Renewable energy sources and environmentally friendly vehicles, Publishing House WNT, Warsaw, 2007 (in Polish).
[2] J. Peng, L. Lu, H. Yang, Review on life cycle assessment of energy payback and greenhouse gas emission of solar photovoltaic systems, Renewable and Sustainable Energy Reviews 19 (2013) 255-274.
[3] L.A. Dobrzański, A. Drygała, M. Giedroć, Application of crystalline silicon solar cells in photovoltaic modules, Archives of Materials Science and Engineering 44/2 (2010) 96-103.
[4] L.A. Dobrzański, A. Drygała, M. Giedroć, M. Macek, Monocrystalline silicon solar cells applied in photovoltaic system, Journal of Achievements in Materials and Manufacturing Engineering 53/1 (2012) 7-13.
[5] L.A. Dobrzański, Engineering Materials and material design: the basis learning about materials and metal science, Scientific and Technical Publishing House, Warsaw, 2006.
[6] M.A. Green, K. Emery, Y. Hishikawa, W. Warta, E.D. Dunlop, Solar cell efficiency tables (version 39), Progress in Photovoltaics: Research and Applications 20/1 (2012) 12-20.
[7] D. Yang, P. Wang, X. Yu, D. Que, Germanium-doped crystalline silicon, A new substrate for photovoltaic application, Journal of Crystal Growth 362 (2013) 140-144.
[8] D. Hocinea, M.S. Belkaid, M. Pasquinelli, L. Escoubas, J.J. Simon, G.A. Rivière, A. Moussi, Improved efficiency of multicrystalline silicon solar cells by $TiO_2$ antireflection coatings derived by APCVD process, Materials Science in Semiconductor Processing 16/1 (2013) 113-117.
[9] M. Wright, A. Uddin, Organic - inorganic hybrid solar cells, A comparative review, Solar Energy Materials and Solar Cells 107 (2012) 87-111.
[10] A. Goetzberger, C. Hebling, Photovoltaic materials, past, present, future, Solar Energy and Solar Cells 62 (2000) 1-19.
[11] G.H. Lee, Ch.K. Rhee, K.S. Lim, A study on the fabrication of polycrystalline Si wafer by direct casting for solar cell substrate, Solar Energy 80 (2006) 220-225.
[12] M. Ju, M. Gunasekaran, K. Kim, K. Han, A new vapour texturing method for multicrystalline silicon solar cell applications, Materials Science and Engineering B 153 (2008) 66-69.
[13] J.S. Yoo, I.O. Pam, Black silicon layer formation for application in solar cells, Solar Energy Materials and Solar Cells 90 (2006) 3085-3093.
[14] C. Xiao, D. Yang, X. Yu, P. Wang, P. Chen, D. Que, Effect of dopant compensation on the performance of Czochralski silicon solar cells, Solar Energy Materials and Solar Cells 101 (2012) 102-106.
[15] S.Y. Lim, D. Macdonald, Measuring dopant concentrations in p-type silicon using iron-acceptor pairing monitored by band-to-band photoluminescence, Solar Energy Materials and Solar Cells 95/8 (2011) 2485-2489.
[16] K. Shirasawa, Mass production technology for multicrystalline Si solar cells, Current Applied Physics 1 (2001) 509-514.
[17] L.A. Dobrzański, M. Musztyfaga, Effect of the front electrode metallisation process on electrical parameters of a silicon solar cell, Journal of Achievements in Materials and Manufacturing Engineering 48/2 (2011) 115-144.
[18] L.A. Dobrzański, M. Musztyfaga, A. Drygała, P. Panek, Investigation of the screen printed contacts of silicon solar cells from Transmissions Line Model, Journal of Achievements in Materials and Manufacturing Engineering 41/1-2 (2010) 57-65.
[19] L.A. Dobrzański, M. Musztyfaga, A. Drygała, P. Panek, Electrical and optical properties of photovoltaic cells manufactured using screen printing methods, Electronics - Design, Technology, Applications 5 (2010) 63-65.
[20] L.A. Dobrzański, M. Musztyfaga, A. Drygała, P. Panek, K. Drabczyk, P. Zięba, Manufacturing photovoltaic solar cells using the screen printing method, Proceeding of the 1st National PV Conference, Krynica-Zdrój, 2009,1-9.
[21] L.A. Dobrzański, M. Musztyfaga, M. Staszuk, Metallisation technology of silicon solar cells using the convectional and laser technique, Proceeding of the 14th International Materials Symposium IMSP'2012, 2012, 155.
[22] L.A. Dobrzański, M. Musztyfaga, A. Drygała, Comparison of conventional and unconventional methods for the front side metallization of silicon solar cells, Proceeding of the 14th International Conference on Advances in "Materials And Processing Technologies" AMPT 2011, 2012, 284.
[23] L.A. Dobrzański, M. Musztyfaga, A. Drygała, A comparative study of both selective laser sintered and screen printed front contacts on monocrystalline silicon solar cells, Mechanics and informatics, Proceeding of the VIII Ukrainian-Polish Conference for Young Researches, Ukraine, 2011, 168-170.
[24] M.W.P.E. Lamers, I.G. Romijn, M. Gagliardo, M.N. van den Donker, C.J.J. Tool, A.W. Weeber, going to a finite source emitter: improved emitter technology by reduction of the dead p-layer for high-efficiency crystalline silicon solar cells, Proceeding of the 23th European Photovoltaic Solar Energy Conference, Valencia, 2008.

[25] Y. Komatsu, A.F. Stassen, P. Venema, A.H.G. Vlooswijk, C. Meyer, M. Koorn, sophistication of doping profile manipulation - emitter performance improvement without additional process step, Proceeding of the 25th European Photovoltaic Solar Energy Conference and Exhibition 5th World Conference on Photovoltaic Energy Conversion Valencia, 2010.

[26] J. Hoornstra, W. Strien, M. Lamers, K. Tool, A. Weeber, High throughput in-line diffusion: emitter and cell results, Proceedings of the 22th European Photovoltaic Solar Energy Conference and Exhibition, Milan, 2007.

[27] A.F. Stassen, M. Koppes, Y. Komatsu, A. Weeber, J. Hoogboom, J. Oosterholt, S. Ritmeijer, L. Groenewoud, Further improvements in surface modification of mc silicon solar cells, Comparison of different post-psg cleans suitable for inline emitters, Proceeding of the 24th European Photovoltaic Solar Energy Conference and Exhibition, Hamburg, 2009.

[28] D. Trusheima, M. Schulz-Ruhtenberga, T. Baierb, S. Krantzc, D. Bauerd, J. Dase, Investigation of the Influence of pulse duration in laser processes for solar cells, Physics Procardia 12 (2011) 278-285.